Assembly of a rod-shaped chimera of a trimeric GCN4 zipper and the HIV-1 gp41 ectodomain expressed in *Escherichia coli*

Winfried Weissenhorn[†‡], Lesley J. Calder[§], Andréa Dessen[†], Tom Laue[¶], John J. Skehel[§], and Don C. Wiley[†‖**††]

[†]Laboratory of Molecular Medicine, and [‡]Howard Hughes Medical Institute, The Children's Hospital, 320 Longwood Avenue, Boston, MA 02215; [§]National Institute for Medical Research, Mill Hill, The Ridgeway, London, NW7 1AA, United Kingdom; [¶]Department of Biochemistry and Molecular Biology, University of New Hampshire, Durham, New Hampshire 03824; and [‖]Department of Molecular and Cellular Biology, and [**]Howard Hughes Medical Institute, Harvard University, 7 Divinity Avenue, Cambridge, MA 02138

ABSTRACT **The HIV-1 envelope subunit gp41 plays a role in viral entry by initiating fusion of the viral and cellular membranes. A chimeric molecule was constructed centered on the ectodomain of gp41 without the fusion peptide, with a trimeric isoleucine zipper derived from GCN4 (pIIGCN4) on the N terminus and part of the trimeric coiled coil of the influenza virus hemagglutinin (HA) HA2 on the C terminus. The chimera pII-41-HA was overexpressed as inclusion bodies in bacteria and refolded to soluble aggregates that became monodisperse after treatment with protease. Either trypsin or proteinase K, used previously to define a protease-resistant core of recombinant gp41 [Lu, M., Blacklow, S. C. & Kim, P. S. (1995) *Nat. Struct. Biol.* 2, 1075–1082], removed about 20–30 residues from the center of gp41 and all or most of the HA2 segment. Evidence is presented that the resulting soluble chimera, retaining the pIIGCN4 coiled coil at the N terminus, is an oligomeric highly α-helical rod about 130 Å long that crystallizes. The chimeric molecule is recognized by the Fab fragments of mAbs specific for folded gp41. A similar chimera was assembled from the two halves of the molecule expressed separately in different bacteria and refolded together. Crystals from the smallest chimera diffract x-rays to 2.6-Å resolution.**

The envelope glycoprotein of HIV-1 is active in receptor binding, cellular tropism, and cell entry through membrane fusion. The glycoprotein is produced as a precursor, gp160, that is posttranslationally cleaved into the subunits gp120 and gp41 (1, 2), an event required for viral infectivity (3). On the viral surface the gp120 subunit is noncovalently associated with gp41. It contains the binding site for the primary cellular receptor CD4 (4, 5) and the coreceptor, a member of the chemokine receptor family (for review, see ref. 6) The gp41 subunit is anchored in the membrane and shows a structural organization common to many viral fusion proteins, including a nonpolar fusion peptide at the N terminus followed by a sequence predicted to form a coiled coil (7–10).

Evidence for the presence of a trimeric coiled coil in gp41, analogous to that found in the fusion-peptide-containing subunit of the influenza virus hemagglutinin (HA) HA2 after induction by low pH (11, 12) and the Moloney murine leukemia virus (MoMuLV) TM subunit (13), has been found in studies of recombinant gp41 (14–16). Electron micrographs indicate that the ectodomain, missing the N-terminal fusion peptide, of recombinant trimeric gp41 secreted from insect cells, is a thin rod-shaped molecule about 120 Å long (16). Biochemical data suggest that a central trimeric coiled coil of N-terminal residues is surrounded by three antiparallel α-he-lices from the C-terminal end (14, 15, 17–19). These data are consistent with the finding that short peptides from the N-terminal and C-terminal regions of gp41 block membrane fusion and thus infection of HIV-1 (20, 21).

Herein we describe the expression, crystallization, and characterization of chimeric molecules containing the ectodomain of HIV-1 gp41. Treatment of the chimeras with trypsin and proteinase K resulted in monodisperse oligomers composed of two segments. Similar molecules were produced by expressing the two halves of the chimeras. Antibody binding, circular dichroism, and electron microscopy provide evidence that the chimeras contain a long coiled coil and retain structural features of viral gp41.

METHODS

Cloning and Protein Expression. The *env* gene sequence for residues 30–167 of gp41 (HXB2 strain) (22) was amplified with synthetic oligonucleotides and both cysteines were mutated to serines by standard PCR methods. DNA encoding GCN4 residues 250–280 with both the a and d position of the coiled coil mutated to isoleucine (pII) (23) was synthesized as two overlapping oligonucleotides. DNA encoding influenza hemagglutinin HA2 residues 43–88 were also amplified with oligonucleotides (with an additional Gly residue, LDG*-43A-HA2; Fig. 1). The three DNA fragments encoding pII, gp41, and HA2 were subcloned into the expression vector pRSET (Invitrogen) (pII41HA) and transformed into *Escherichia coli* cells BL21 DE3/pUBS (24). DNA sequencing revealed the inadvertent insertion of Ile-6 in the HA2 sequence. DNA fragments encoding the N-terminal proteinase K-specific digestion products (pII41N = pII amino acids 250–280 and gp41 amino acids 30–79) and a C-terminal fragment (41HAC = gp41 amino acids 113–157 and HA2 amino acids 43–88) were also subcloned into vector pRSET (Invitrogen) and expressed in *E. coli* BL21 (DE3/pUBS). Mutagenesis of pIIGCN amino acids Asp-6 to Cys and Lys-27 to Cys in the pII41N-Cys construct was performed by standard PCR methods.

Protein Purification and Proteolysis. Bacteria were lysed in PBS by sonication, and insoluble material was pelleted at 40,000 rpm (T.45 rotor, Beckman) for 1 hr. Inclusion bodies (pII-41-HA) were purified by washing the pellet four times with PBS/0.5% Triton X-100 and once in PBS without Triton X-100, solubilized in 8 M urea/PBS, and refolded by dilution into 50 mM Tris (pH 8.5) at 10 μM PII41HA. 7-Amino-1-chloro-3-tosylamido-2-heptanone-treated trypsin (Sigma) or proteinase K (Boehringer Mannheim) digestions [1:200 (wt/wt), 1 hr, 37°C] were quenched with 2 mM phenylmethylsulfonyl fluoride (Sigma). The proteolytic products pII41PT and pII41PK (Fig. 1) were concentrated and purified by gel

Abbreviations: HA, hemagglutinin; MoMuLV, Moloney murine leukemia virus.
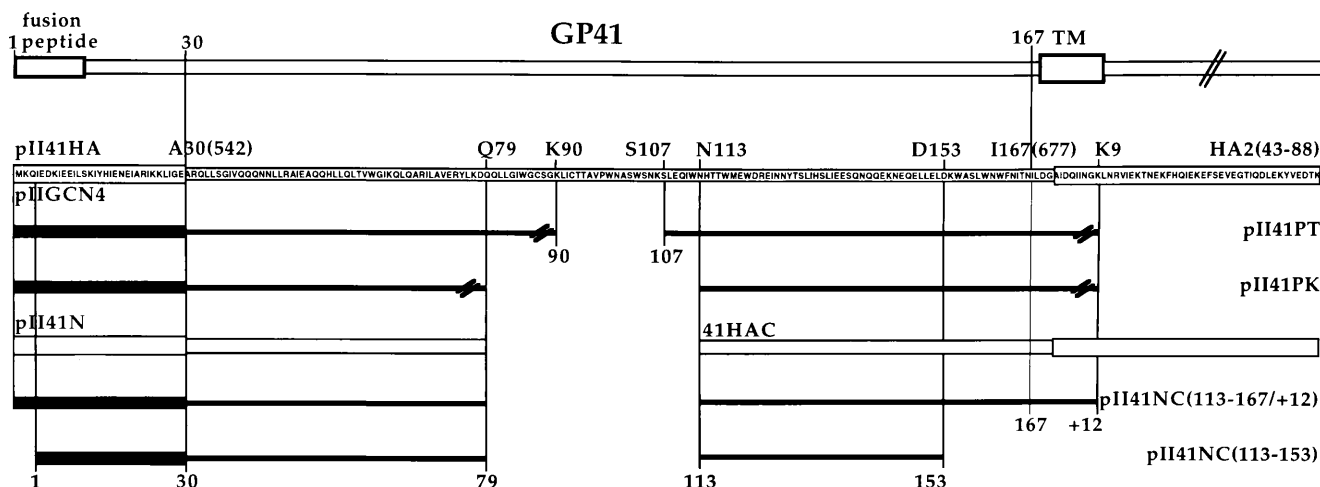[††]To whom reprint requests should be addressed.

FIG. 1.   gp41 constructs and proteins. Sequences of construct pII-41-HA and schematic drawings of the protease digestion products pII41PT and pII41PK and the two pII41NC constructs are shown. Solid bars are characterized proteins; open bars are expression constructs. The cysteine codons in expression construct pII41HA were changed to serine (residue positions 87 and 93).

filtration chromatography with Superdex 200 (Pharmacia) (20 mM Hepes, pH 8.3/75 mM NaCl).

An equimolar mixture of pII41N and 41HAC (10 mM each) was refolded by dilution into 50 mM Tris (pH 8.5). Trypsin (Sigma) treatment of the soluble aggregates [1:500 (wt/wt), 37°C, 1 hr] was quenched with 2 mM phenylmethylsulfonyl fluoride (Sigma). PII41NC complexes were purified by Superdex 200 gel filtration chromatography (Pharmacia) (20 mM Hepes pH 8.3/75 mM NaCl). PII41NC-Cys was reconstituted as described for pII41NC with 10 mM dithiothreitol in all the buffers. PII41NC(113–167/+12) and pII41NC(113–153) (Fig. 1) were purified by reversed-phase FPLC (Pharmacia Pro-RPC) using a linear gradient of acetonitrile containing 0.2% trifluoroacetic acid. Electrospray ionization mass spectrometry was performed on a Finnigan TSQ7000 triple quadruple spectrometer.

Chemical Cross-linking. The buffer of pII41NC-Cys(113–153) (1 mg/ml) was changed to 50 mM sodium phosphate/150 mM NaCl prior to cross-linking with bismaleimidohexane (Pierce) at room temperature for 30 min. The reactions were quenched with 100 mM dithiothreitol and the cross-linked products were analyzed by Tricine gel electrophoresis (15% gels) (25).

Sedimentation Equilibrium Analysis. Short-column sedimentation equilibrium experiments in charcoal-filled Epon centerpieces were carried out in a Beckman model XL1 analytical ultracentrifuge equipped with Rayleigh interference optics at rotor speeds of 15,000, 20,000, 25,000, 30,000 and 35,000 rpm at concentrations ranging from 0.1 to 2.0 mg/ml (20 mM Hepes, pH 8.35/74 mM NaCl). The data collected from the experiments were truncated to avoid Weiner skewing at high-fringe gradient or noisy data at low-fringe gradients by using the program REEDIT. The data were then analyzed with the program NONLIN, which provides fitting parameters and the limits for 95% confidence intervals. The trimer model had the best variance of fit and an acceptably random distribution of residuals. A partial specific volume of 0.7415 was calculated from the amino acid composition.

Fabs. Fab fragments of mAbs 2A2 (Repligen) and D36 (26) were generated as described (16) and separated from Fc fragments by protein A column chromatography (Bio-Rad). For gel-shift experiments, pII41PT, pII41NC(113–153), and pII41NC(113–167/+12) (all at 2 mg/ml) were mixed with Fab fragments (20 mM Hepes, pH 8.0/100 mM NaCl) at equimolar concentrations and separated on 8–25% gradient gels (Pharmacia Phast Gel System) under native conditions and stained with Coomassie brilliant blue.

Electron Microscopy. Samples were adsorbed onto carbon films, negatively stained with 1% sodium silcotungstate (pH 7.0), and examined with a JEOL 1200EX microscope at 100 kV as described (16).

RESULTS

Expression, Refolding, Proteolysis, and Crystallization of the gp41 Chimera. Residues 30–167 of the extracellular region of gp41, lacking the N-terminal fusion peptide (Fig. 1), were expressed as a fusion protein in *E. coli*. The construct contains 31 residues of a mutated GCN4 dimerization domain, pII, at the N terminus. Heptad positions a and d in the GCN4 coiled coil were changed to isoleucine, which has been shown to favor formation of a trimeric coiled coil (23). The GCN4 heptads were placed in register with a proposed coiled coil segment in gp41 (8, 9, 27). In addition, a coiled-coil domain (amino acids 43–88) of the influenza virus HA subunit HA2 in the low-pH-induced conformation (11) was placed C-terminal to the gp41 residues, effectively replacing the transmembrane anchor (Fig. 1, pII41HA). This gp41 chimera is highly overexpressed in *E. coli* despite the inadvertent insertion of Ile at position 5 of the HA2 sequence and forms insoluble inclusion bodies.

The inclusion bodies were purified and solubilized in urea. *In vitro* refolding yielded soluble protein that was aggregated, as judged by gel filtration chromatography. Protease treatment with trypsin or proteinase K resulted in a soluble monodisperse molecule composed of two segments that migrate as approximately 6.5-kDa and 4.5-kDa bands on SDS/Tricine gel electrophoresis (Fig. 2). N-terminal sequencing of the 6.5-kDa bands identified the sequence of the pIIGCN4 at the N terminus of both the trypsin and the proteinase K digestion products (Fig. 1, pII41PT and pII41PK). The N terminus of the
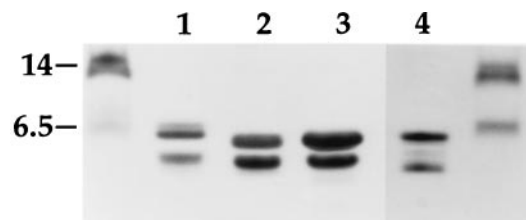

FIG. 2.   Tricine SDS/PAGE of proteolytic products. Lanes: 1, pII41PT; 2, pII41PK; 3, pII41NC(113–167/+12); 4, pII41NC(113–153). Molecular weight standards are shown and bands are visualized with Coomassie brilliant blue staining.

smaller, approximately 4.5-kDa, components were identified as Ser-107 of gp41 for the trypsin digestion (Fig. 1, pII41PT) and Asn-113 of gp41 for the proteinase K digestion (Fig. 1, pII41PK). These N termini have been described as boundaries of a protease-resistant core of recombinant gp41 generated in bacteria (14).

Both the proteinase K digestion product pII41PK and the trypsin product pII41PT crystallized readily into small rod-shaped crystals.

Assembly of a gp41 Chimera from Two Halves. In an attempt to avoid protease treatments, N- and C-terminal segments, pII41N [pII+gp41(30–79)] and 41C [gp41(113–157)], were expressed separately, but only the N-terminal part (pII41N) was overexpressed (Fig. 1). A second C-terminal construct 41HAC [gp41(113–167)+HA2(43–88) containing an Ile-6 insertion in the HA2 sequence] was also expressed and refolded with the N-terminal segment, pII41N (Fig. 1). Treatment of the product with trypsin resulted in two monodisperse gp41 chimeras, pII41NC(113–167/+12) and pII41NC(113–153) (Figs. 1 and 2, lanes 3 and 4), depending on the extent of trypsin treatment. The composition of the chimeras has been determined by N-terminal sequencing and mass spectrometry. pII41NC(113–167/+12) contains pII-GCN4(1–30)+gp41(30–79) as the N-terminal fragment (mass observed, 9517.2; calculated, 9503.0) and gp41(113–167/+12) (mass observed, 7874.3; calculated, 7875.6) as the C-terminal fragment. [The SDS/Tricine gel mobility of the C-terminal fragment of pII41NC(113–167/+12) is similar to the C-terminal fragments of pII41PT and pII41PK (Fig. 2, lanes 1–3), suggesting that those constructs share the same or a similar C terminus.] More extensive trypsin digestion resulted in a shorter chimera pII41NC(113–153) containing pII-GCN4 (3–30)+gp41(30–79) as the N-terminal fragment (mass observed, 9257.0; calculated, 9259.8) and gp41(113–153) (mass observed, 5190.6; calculated, 5192.2) as the C-terminal fragment. pII41NC(113–167/+12) formed small cube-shaped crystals from ammonium sulfate solutions and the pII41NC(113–153) formed hexagonal-shaped crystals from magnesium acetate, ammonium sulfate, and sodium citrate solutions. The latter crystals diffract x-rays to 2.6-Å resolution.

Oligomeric State. Chemical cross-linking indicated a trimeric oligomeric state. A sulfhydryl reactive cross-linker was reacted with pII41NC-cys, which contains two free cysteines in the N-terminal pIIGCN sequence of the pIINC(113–153) molecule (Fig. 1). With the exception of the engineered cysteines pII41NC-cys is identical to pII41NC(113–153) and is refolded and solubilized by proteolysis in the same way. After cross-linking, two new bands appear (Fig. 3, lanes 4 and 5), migrating at 16 and 22 kDa, corresponding to a dimeric and trimeric form of the N-terminal fragment pII41N of the molecule pII41NC (113–153). pII41NC(113–153) without cys-

teines was not cross-linked under the same conditions (data not shown).

A trimeric organization of pII41NC(113–153) (monomer, 14.4 kDa) is also supported by the molecular weight measured by sedimentation equilibrium centrifugation. The average molecular weight for four protein loading concentrations and five rotor speeds was 47.9, 45.8, 41.8, 38.2, and 45.2 kDa, without a systematic decrease in the molecular weight as the rotor speed increased, indicating a sample free of aggregates. The lack of a systematic decrease in the molecular weight with dilution suggests that the absence of a monomer–oligomer equilibrium at the concentrations used. The data were fit best by a trimer of pII41NC (calculated, 43.2 kDa).

Binding of gp41-Specific Antibodies. Native gel electrophoresis was used to test the binding of Fab fragments from gp41-specific mAbs to the gp41 chimeras. mAb 2A2 has been mapped to the N-terminal (K. Javaharian, personal communication) and mAb D36 to the C-terminal part of the gp41 ectodomain (26). Both Fab fragments bind to pII41PT and shift its mobility. Fig. 4*a* shows that Fab D36 shifts the mobility of pII41PT (lanes 1–3). Binding of Fab 2A2 is also observed (Fig. 4*a*, lanes 3 and 4). The chimeras missing residues 80–90 of the N-terminal segment pII41PK (data not shown), pII41NC(113–167/+12) (Fig. 4*b*), and pII41NC(113–153) (Fig. 4*c*) bind only Fab D36, which recognizes the C-terminal region of gp41 (Fig. 4 *b* and *c*, lanes 1–3). No shift in mobility is observed with the N-terminal-specific Fab 2A2 for these chimeras (Fig. 4 *b* and *c*, lanes 4 and 5) that all lack residues 79–90, implying that amino acids 79–90 of gp41 are required for binding Fab 2A2.

Evidence of High α-Helical Content and a Rod-Like Structure. The CD spectra of pII41PT was measured from 190 nm to 250 nm, yielding a calculated α-helical content of ≈94%.

Electron microscopy of pII41PT (Fig. 5) and pII41NC(113–153) (data not shown) clearly shows a rod-like structure. Measurement of 70 molecules indicated an average length of about 12.9 nm for pII41PT and 12.5 nm for pII41NC(113–153). This is approximately the length expected for an α-helical coiled coil spanning the 90 residues from the N-terminal end of the GCN4 segment to residue 90 of gp41 at the trypsin cleavage site (Fig. 1, pII41PT). Subtracting the calculated length of the GCN4 coiled-coil domain (31 amino acids) suggests that the gp41 core (residues 30–90 and 107–167/[+12]) contributes about 8.3 nm to the length of the chimeric molecule.

DISCUSSION

GCN4–gp41 chimeras that are oligomeric, soluble, monodisperse, and crystalline were produced by bacterial expression and protease treatment to extend the description of the structure of the gp41 subunit of the HIV-1 envelope glycoprotein. The addition of a polar N-terminal GCN4 extension,
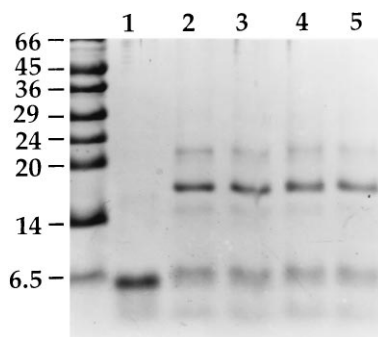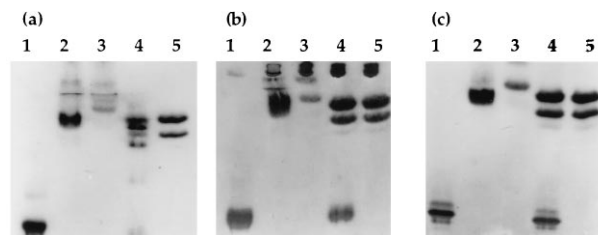

FIG. 3. Chemical cross-linking of pII41NC-cys. Cross-linked products were separated on 15% Tricine SDS/PAGE gels and bands are stained with Coomassie brilliant blue. The bismaleimidohexane concentrations are as follows. Lanes: 1, no bismaleimidohexane; 2, 0.5 mM; 3, 1.0 mM; 4, 2 mM; 5, 5 mM. Molecular weight standards are shown.

FIG. 4. Native gel electrophoresis band-shift assay of Fab binding (8–25% Phast gel). Bands are stained with Coomassie brilliant blue. (*a*) Lanes: 1, pII41PT; 2, pII41PT and Fab D36; 3, Fab D36; 4, pII41PT and Fab 2A2; 5, Fab 2A2. (*b*) Lanes: 1, pII41NC(113–167/+12); 2, pII41NC and Fab D36; 3, Fab D36; 4, pII41NC and Fab 2A2; 5, Fab 2A2. (*c*) Lanes: 1, pII41NC(113–153); 2, pII41NC and Fab D36; 3, Fab D36; 4, pII41NC and Fab 2A2; 5, Fab 2A2.
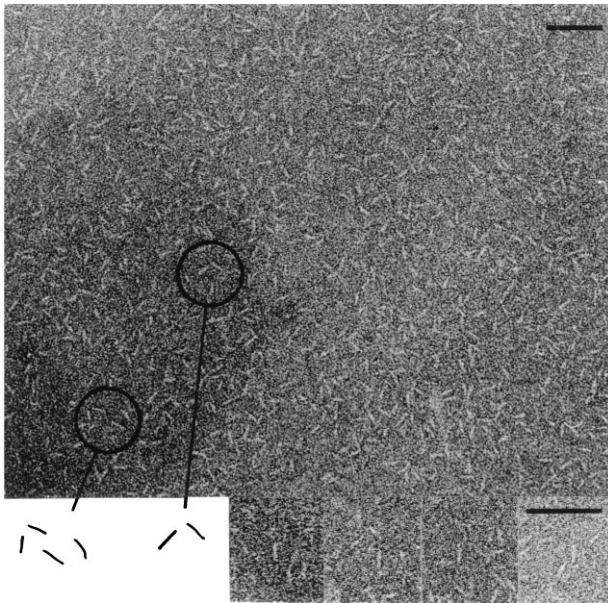
FIG. 5.   Electron micrographs of pII41PT. Diagrammatic representations of the molecules are shown. The average length of the rods is 12.9 nm.

replacing the fusion peptide in gp41, substantially increased the solubility of gp41 relative to similar molecules without the GCN4 expressed inside bacteria (W.W., unpublished observations) or secreted as a glycosylated oligomer from insect cells (16).

A number of observations suggest that the gp41 chimeras are folded like the ectodomain of viral gp41. The chimeras have a high α-helical content and a long thin rod shape, all features shared by influenza HA$_2$ from virus after activation by low pH (11, 28, 29) or expressed in *E. coli* (30) and MoMuLV TM expressed as a soluble segment in *E. coli* (13, 31). The similarity of these properties of the chimera to those of the ectodomain of gp41 (with fusion peptide deleted) secreted from insect cells, including nearly identical images in the electron microscope (figure 6a in ref. 16), suggests that the GCN4 addition only lengthened, stabilized, and made more soluble the same folded structure that was found in gp41 alone. pII41PT (Fig. 1) was also shown to bind Fabs from two mAbs specific for gp41. The chimera could be produced intact or from its two halves (Fig. 1) and the central portion of about 30 residues is removed by protease, both properties of recombinant gp41 ectodomain segments, gp41(29–158) of simian immunodeficiency virus and HIV-1 expressed in bacteria (14, 15).

The gp41 chimeras appear to be trimeric like the ectodomain of gp41 with the fusion peptide deleted as expressed in insect cells (16), the protease-resistant core of the gp41 segment, residues 29–158 (14, 15), the influenza virus HA (32), and the MoMuLV retrovirus envelope glycoprotein fusion subunit (13). Chemical cross-linking of pII41NC-cys showed two new bands migrating at approximately 16 and 22 kDa, close to two and three times the sum of the N-terminal peptide pII41N (9.2 kDa). The C-terminal fragment is not cross-linked under these conditions. [The component peptides of the chimeras migrate anomalously on SDS/PAGE, however; the bands migrating near markers at 6.5 kDa and less are peptides of 9–10 kDa (N terminus) and 7.8 or 5.2 kDa (C terminus), respectively. This anomalous migration of the short component peptides of the protease-resistant core of gp41 has been observed (14)]. In addition sedimentation equilibrium centrifugation of pII41NC(13–153) indicates a trimeric organization consistent with earlier observations (14, 19). An independent reason for thinking that the chimeras are trimeric is that the pIIGCN4

segment on the N-terminal ends form stable triple-stranded α-helical coiled coils even on their own (33).

The length of the gp41 chimera measured by electron microscopy, about 130 Å, is that expected for a structure that is an α-helical coiled coil from the N-terminal GCN4 sequence to near residue 90 of gp41 (Fig. 1). The electron microscopy herein and in Weissenhorn *et al.* (16) of the ectodomain of gp41 expressed in insect cells, which describe thin rods similar to electron microscopic images of the influenza HA$_2$ coiled coil containing structure (28–30) provides direct evidence for models of gp41 containing a long coiled coil (14–16, 20, 34). The similarity of the gp41 structure to that found in other viral membrane fusion proteins such as influenza virus and Mo-MuLV argues for a similarity in the mechanisms of membrane fusion during viral entry, even though the triggering events leading to the activation of membrane fusion are different.

mAb 2A2, previously shown by electron microscopy to bind to one end of the rod-like gp41 ectodomain expressed in insect cells (figure 6b in ref. 16), in the present work was shown to require gp41 residues 79–90 for recognition of gp41 chimeras (Figs. 1 and 3). This is consistent with the rod-shaped gp41 chimera and gp41 from insect cells having residue 90 near one end of a central coiled coil, an arrangement also proposed from protease digestion experiments for the protease-resistant core of recombinant simian immunodeficiency virus and HIV-1 gp41 (14, 15). Our proteolysis data are consistent with the antiparallel placement of the C-terminal segment as proposed from protease data and analysis of sequence conservation for recombinant simian immunodeficiency virus and HIV-1 (14, 15). The mapping of mAb 2A2 should allow comparison of the structure of recombinant gp41 and viral gp41 in its various conformational states.

The crystals obtained with the chimera pII41NC(113–153) should allow the structure to be determined at atomic resolution. Adding a GCN4 segment to gp41 expressed in insect cells might produce chimeras that would include the 34 residues from the middle part of the sequence, which contains two additional oligosaccharide sites and a short disulfide loop that forms an immunodominant region (35) implicated in a conformational change (16) after CD4 and chemokine receptor binding.

1. Allan, J. S., Coligan, J. E., Barin, F., McLane, M. F., Sodroski, J. G., Rosen, C. A., Haseltine, W. A., Lee, T. H. & Essex, M. (1985) *Science* **228,** 1091–1094.
2. Veronese, F. D., DeVico, A. L., Copeland, T. D., Oroszlan, S., Gallo, R. C. & Sarngadharan, M. G. (1985) *Science* **229,** 1402–1405.
3. McCune, J. M., Rabin, L. B., Feinberg, M. B., Lieberman, M., Kosek, J. C., Reyes, G. R. & Weissman, I. L. (1988) *Cell* **53,** 55–67.
4. Dalgleish, A. G., Beverley, P. C., Clapham, P. R., Crawford, D. H., Greaves, M. F. & Weiss, R. A. (1984) *Nature (London)* **312,** 763–767.
5. Klatzmann, D., Champagne, E., Chamaret, S., Gruest, J., Guetard, D., Hercend, T., Gluckman, J. C. & Montagnier, L. (1984) *Nature (London)* **312,** 767–768.
6. Wilkinson, D. (1996) *Curr. Biol.* **6,** 1051–1053.
7. Bosch, M. L., Earl, P. L., Fargnoli, K., Picciafuoco, S., Giombini, F., Wong-Staal, F. & Franchini, G. (1989) *Science* **244,** 694–697.
8. Chambers, P., Pringle, C. R. & Easton, A. J. (1990) *J. Gen. Virol.* **71,** 3075–3080.

9. Gallaher, W. R., Ball, J. M., Garry, R. F., Griffin, M. C. & Montelaro, R. C. (1989) *AIDS Res. Hum. Retroviruses* **5,** 431–440.
10. Kowalski, M., Potz, J., Basiripour, L., Dorfman, T., Goh, W. C., Terwilliger, E., Dayton, A., Rosen, C., Haseltine, W. & Sodroski, J. (1987) *Science* **237,** 1351–1355.
11. Bullough, P. A., Hughson, F. M., Skehel, J. J. & Wiley, D. C. (1994) *Nature (London)* **371,** 37–43.
12. Carr, C. M. & Kim, P. S. (1993) *Cell* **73,** 823–832.
13. Fass, D., Harrison, S. C. & Kim, P. S. (1996) *Nat. Struct. Biol.* **3,** 465–469.
14. Lu, M., Blacklow, S. C. & Kim, P. S. (1995) *Nat. Struct. Biol.* **2,** 1075–1082.
15. Blacklow, S. C., Lu, M. & P. S., K. (1995) *Biochemistry* **34,** 14955–14962.
16. Weissenhorn, W., Wharton, S. A., Calder, L. J., Earl, P. L., Moss, B., Aliprandis, E., Skehel, J. J. & Wiley, D. C. (1996) *EMBO J.* **15,** 1507–1514.
17. Chen, C. H., Matthews, T. J., McDanal, C. B., Bolognesi, D. P. & Greenberg, M. L. (1995) *J. Virol.* **69,** 3771–3777.
18. Lawless, M. K., Barney, S., Guthrie, K. I., Bucy, T. B., Petteway, J., S. R. & Merutka, G. (1996) *Biochemistry* **35,** 13697–13708.
19. Rabenstein, M. D. & Shin, Y.-K. (1996) *Biochemistry* **35,** 13922–13928.
20. Wild, C. T., Oas, T., McDanal, C. B., Bolognesi, D. & Matthews, T. (1992) *Proc. Natl. Acad. Sci. USA* **89,** 10537–10541.
21. Wild, C. T., Shugars, D. C., Greenwell, T. K., McDanal, C. B. & Matthews, T. J. (1994) *Proc. Natl. Acad. Sci. USA* **91,** 9770–9774.
22. Fisher, A. G., Collalti, E., Ratner, L., Gallo, R. C. & Wong-Staal, F. (1985) *Nature (London)* **316,** 262–265.
23. Harbury, P. B., Zhang, T., Kim, P. S. & Alber, T. (1993) *Science* **262,** 1401–1407.
24. Brinkmann, U., Mattes, R. E. & Buckel, P. (1989) *Gene* **85,** 109–114.
25. Schagger, H. & von Jagow, G. (1987) *Anal. Biochem.* **166,** 368–379.
26. Earl, P. L., Broder, C. C., Long, D., Lee, S. A., Peterson, J., Chakrabarti, S., Doms, R. W. & Moss, B. (1994) *J. Virol.* **68,** 3015–3026.
27. Delwart, E. L., Mosialos, G. & Gilmore, T. (1990) *AIDS Res. Hum. Retroviruses* **6,** 703–706.
28. Ruigrok, R. W., Aitken, A., Calder, L. J., Martin, S. R., Skehel, J. J., Wharton, S. A., Weis, W. & Wiley, D. C. (1988) *J. Gen. Virol.* **69,** 2785–2795.
29. Wharton, S. A., Calder, L. J., Ruigrok, R. W., Skehel, J. J., Steinhauer, D. A. & Wiley, D. C. (1995) *EMBO J.* **14,** 240–246.
30. Chen, J., Wharton, S. A., Weissenhorn, W., Calder, L. J., Hughson, F. M., Skehel, J. J. & Wiley, D. C. (1995) *Proc. Natl. Acad. Sci. USA* **92,** 12205–12209.
31. Fass, D. & Kim, P. S. (1995) *Curr. Biol.* **5,** 1377–1383.
32. Wiley, D. C., Skehel, J. J. & Waterfield, M. (1977) *Virology* **79,** 446–448.
33. Harbury, P. B., Kim, P. S. & Alber, T. (1994) *Nature (London)* **371,** 80–83.
34. Bernstein, H. B., Tucker, S. P., Kar, S. R., McPherson, S. A., McPherson, D. T., Dubay, J. W., Lebowitz, J., Compans, R. W. & Hunter, E. (1995) *J. Virol.* **69,** 2745–2750.
35. Xu, J. Y., Gorny, M. K., Palker, T., Karwowska, S. & Zolla-Pazner, S. (1991) *J. Virol.* **65,** 4832–4838.-